Charge fluctuations in a perfect and disturbed quantum wire

2006 J. Phys.: Condens. Matter 18 7313

(http://iopscience.iop.org/0953-8984/18/31/024)

INSTITUTE OF PHYSICS PUBLISHING JOURNAL OF PHYSICS: CONDENSED MATTER

J. Phys.: Condens. Matter **18** (2006) 7313–7326 doi:10.1088/0953-8984/18/31/024

Charge fluctuations in a perfect and disturbed quantum wire

T Kwapiński

Institute of Physics and Nanotechnology Center, M Curie-Skłodowska University, 20-031 Lublin, Poland

E-mail: tomasz.kwapinski@umcs.lublin.pl

Received 21 February 2006, in final form 23 June 2006
Published 21 July 2006
Online at stacks.iop.org/JPhysCM/18/7313

Abstract

The tight-binding Hamiltonian and retarded Green function formalism are used to study the local and total density of states of a monatomic quantum wire. An additional atom (adatom) can be coupled with the wire at its side. Also the local and average charges of the perfect and disturbed wire are shown and the analytical formula for the local density of states at each site is obtained. The local density of states at each atom in a wire which consists of an even number of atoms is characterized by minima at the Fermi level, in comparison with a wire disturbed by an adatom, where the density of states is characterized by local peaks. Charge fluctuations (waves) are observed in the wire for the case when the condition for the conductance oscillations is satisfied. For the single electron energies of a wire localized above the Fermi energy the local charge along the wire forms a wave curve which possesses one maximum less than for energies localized below the Fermi level.

(Some figures in this article are in colour only in the electronic version)

1. Introduction

Recently, due to the rapid progress in nanotechnology, electron transport through one-dimensional systems has been the subject of active theoretical and experimental research. Monatomic quantum wires are fundamental blocks for nanoelectronic devices; thus it is important to know their electronic properties. The knowledge of these properties is crucial for the fabrication of nanosystems. Such one-dimensional wires can be formed using for example scanning tunnelling microscope (STM) methods [1], the mechanically controlled break junction (MCBJ) [2, 3] or on vicinal surfaces [4–7].

The electronic properties of quantum wires (QWs) have been investigated theoretically and many interesting phenomena have been found; see e.g. [3]. One of them is the even–odd conductance oscillations [8–12]. The value of the conductance oscillates when the number

of atoms in the wire is changed. Also, oscillations with period greater than two have been predicted theoretically [13, 14]. Other interesting phenomena concerning one-dimensional systems are spin–charge separation [15], spontaneous spin polarization [16–18] or conductance quantization [19]. The adsorption on an infinite wire of a single hydrogen or oxygen atom was investigated theoretically in [20] and experimentally in [21], and the results indicate that the conductance is blocked in the presence of such atoms. Also an extended cluster of atoms connected to an infinite atomic chain was studied in [22]. The electrical conductance of an infinite wire with a side-coupled quantum dot (QD) array was investigated theoretically in [23]. The authors concentrated on the influence of the length of a QD array on the conductance through the wire.

The charge distribution in a quantum wire determines its electronic properties. Using a first-principles density-functional method the excess Mulliken charge for different atoms in linear chains was obtained in [24]. For a gold (Au) chain strong charge transport was observed and the chain end atoms gained an extra electron charge due to the difference between the lead and chain work functions. Also, the number of electrons occupying the even and odd QW states are correlated with the resistance of a symmetric molecule [25]. The charge filling of the QW results in the periodicity of the conductance and these periods are determined by the inverse of the conduction band filling [13]. The average charge of a wire oscillates with the wire length (with the same period as the conductance) but for an infinite length it tends to a constant value [13, 14]. Neither of the papers mentioned above have described the charge oscillations inside a wire, and only non-disturbed wires were taken into consideration.

In this paper we are interested in the density of states and charge distribution in a perfect wire and in a wire disturbed by a side-attached adatom. The additional atom can modify the electron properties of the wire depending on the kind of adatom and the coupling with QW. We focus on the analytical solutions for the local density of states (LDOS) at the wire sites in a perfect wire and in the presence of an adatom on it. The knowledge of the LDOS enables us to obtain the local and average charges in the wire. The tight-binding Hamiltonian and Green function method are used in our calculations. The local and total density of states and the formation of the charge waves in a perfect wire are discussed. Also the influence of an adatom on these quantities is analysed.

The paper is arranged as follows. In section 2 the Hamiltonian for a perfect and disturbed wire is presented and the theoretical expressions for the conductance are obtained. In section 3 the numerical results are shown. The discussion of the obtained results is included in sections 3.1 (perfect wire) and 3.2 (disturbed wire). In section 4 some general conclusions are presented.

2. Theoretical description

Our model system—a quantum wire connected to metallic leads with a side-attached atom (adatom)—is described by the following tight-binding Hamiltonian $H = H_{\mathrm{wire}} + H'$, where H_{wire} corresponds to the non-disturbed QW:

$$H_{\mathrm{wire}} = \sum_{\vec{k}\alpha=L,R} \varepsilon_{\vec{k}\alpha} a^{\dagger}_{\vec{k}\alpha} a_{\vec{k}\alpha} + \sum_{n=1}^{N} \varepsilon_n a^{\dagger}_n a_n + \sum_{\vec{k}L,\vec{k}R} V_{\vec{k}L(R)} a^{\dagger}_{\vec{k}L(R)} a_{1(N)} + \sum_{n=1}^{N-1} V_n a^{\dagger}_n a_{n+1} + \mathrm{h.c.} \quad (1)$$

and H' describes the adatom energy, $H' = \varepsilon_x c^{\dagger}_x c_x + t c^{\dagger}_x a_l + \mathrm{h.c.}$ For simplicity a single orbital per site and only the nearest-neighbour interactions are assumed. Here the operators $a_{\vec{k}\alpha}(a^{\dagger}_{\vec{k}\alpha})$, $a_n(a^{\dagger}_n)$ and $c_x(c^{\dagger}_x)$ are the electron annihilation (creation) operators in the lead α ($\alpha = L, R$), at atomic site n ($n = 1, \ldots, N$) and at the adatom, respectively. The hopping parameter

$V_{\vec{k}L(R)}$ is the electron tunnelling coupling between the electron states in the left (right) reservoir and the first (last) atom and $t(V_n)$ is the hopping integral between the electron state of the adatom and the QW atom (nth and $(n+1)$th QW atoms). As we are not interested in many-body effects, e.g. the Kondo effect, the electron–electron correlations are neglected in the first step. This assumption is quite reasonable in some one-dimensional systems, especially for non-magnetic atoms [14, 23]. The neglecting of the Coulomb interactions is justified when the broadening due to electron–electron interactions within the wire is less than the broadening of the molecular levels [25] and for example the electronic structure of alkali nanowires is well described in terms of free and independent electrons [26]. Moreover, the electron–electron correlation does not change the period of conductance oscillations and when the single electron energies correspond to the Fermi energy the even–odd conductance oscillations are the same as for $U = 0$ [18].

The following notation is used in the paper: the capital letter N expresses the length of the wire, the small letter n indicates the number of an atom in the wire $n \in (1, \ldots, N)$ and the index l corresponds to the QW atom which is coupled with an adatom $l \in (1, \ldots, N)$. We can find the local charge at zero temperature localized at QW atoms from the retarded Green function, G^r_{nn}, using the following relation:

$$Q_n = \frac{-1}{\pi} \int_{-\infty}^{E_{\mathrm{F}}} \mathrm{Im}\, G^r_{\mathrm{nn}}(E)\, \mathrm{d}E = \int_{-\infty}^{E_{\mathrm{F}}} \mathrm{LDOS}_n(E)\, \mathrm{d}E \tag{2}$$

where LDOS_n means the local density of states at site n. Next, we assume the symmetric case $\Gamma^L = \Gamma^R = \Gamma$ (where $\Gamma^{L(R)} = 2\pi \sum_{\vec{k}} |V_{\vec{k}L(R)}|^2 \delta(E - \epsilon_{\vec{k}L(R)})$) and consider the same electron energies of all atoms in the wire, i.e. $\varepsilon_i = \varepsilon_0$, and the same coupling strengths between the nearest-neighbour electron states in the wire, $V_n = V_N$. These assumptions are reasonable as we concentrate on the zero or very small source–drain voltage regime and take into consideration the wire which consists of the same kind of atoms.

We can write the general matrix equation for the retarded Green function as follows: $(EI - H^{-1}) \cdot G(E) = A^{N+1} \cdot G(E) = I$, where I is the unit matrix and the matrix A^{N+1} can be written in the form

$$\begin{aligned} A^N_{i,j} &= (E - \varepsilon_0)\delta_{i,j} - V_N(\delta_{i,j+1} + \delta_{i+1,j}) + \mathrm{i}\frac{\Gamma}{2}(\delta_{i,1}\delta_{1,j} + \delta_{i,N}\delta_{N,j}) \\ A_{k,N+1} &= A_{N+1,k} = (E - \varepsilon_x)\delta_{k,N+1} - t\delta_{k,l}. \end{aligned} \tag{3}$$

Here $i, j \leqslant N$, $k \leqslant N+1$ and A^N_{ij} is an $N \times N$ tridiagonal symmetric matrix. By finding the inverse of the matrix A^{N+1} we can obtain the retarded Green functions $G^r = (A^{N+1})^{-1}$. In our case one can write

$$G^r_{\mathrm{nn}}(E) = \frac{\mathtt{cof} A^{N+1}_{\mathrm{nn}}}{\det A^{N+1}} \tag{4}$$

where $\mathtt{cof} A^{N+1}_{\mathrm{nn}}$ is the algebraic complement of the matrix A^{N+1} (cofactor). Using equations (2)–(4) the local density of states can be expressed in the form

$$\mathrm{LDOS}_n = -\frac{1}{\pi}\,\mathrm{Im}\,\frac{\det B^{n-1}\det B^{N-n} + \frac{t^2}{E-\varepsilon_x}\det B^{\min(l,n)-1}\det A^{|l-n|-1}\det B^{N-\max(l,n)}}{\det A^N + \frac{t^2}{E-\varepsilon_x}\det B^{n-1}\det B^{N-n}} \tag{5}$$

where $\det A^N$ corresponds to a non-disturbed QW and can be obtained fully analytically from the following relation; see [14]:

$$\det(A^N) = \det(A^N_0) + \mathrm{i}\Gamma\det(A^{N-1}_0) - \frac{\Gamma}{2}\det(A^{N-2}_0). \tag{6}$$

The matrix A_0^N corresponds to a wire which is non-coupled to the leads and non-disturbed by the adatom. The determinant of the matrix B in equation (5) can be also expressed by means of the A_0^N matrix, i.e.

$$\det(B^N) = \det(A_0^N) + \mathrm{i}\frac{\Gamma}{2}\det(A_0^{N-1}), \tag{7}$$

with the conditions $\det(A_0^{-1}) = 0$, $\det(A_0^0) = 1$ and $\det(A_0^1) = E - \varepsilon_0$. The determinant $\det(A_0^N)$ can be expressed in terms of Chebyshev polynomials of the second kind, $u(\phi)$, i.e. $\det(A_0^N) = V_N^N u_k(\phi)$, where ϕ plays the role of the Bloch phase $\phi = \arccos(\frac{\varepsilon-\varepsilon_0}{2V_N})$. For $n = l$ (the adatom is coupled with the nth QW atom) equation (5) reduces to

$$\mathrm{LDOS}_n = -\frac{1}{\pi}\,\mathrm{Im}\left(\frac{\det A^N}{\det B^{n-1}\det B^{N-n}} + \frac{t^2}{E-\varepsilon_x}\right)^{-1}. \tag{8}$$

Moreover, as $|\varepsilon_x| \to \infty$ (the single electron energy of the adatom is situated far from the Fermi level) the LDOS does not depend on the adatom parameters, and it can be obtained from the following relation: $\mathrm{LDOS}_n = -\frac{1}{\pi}\,\mathrm{Im}\,\frac{\det B^{n-1}\det B^{N-n}}{\det A^N}$. The local density of states at the QW atom, equation (5) and also equation (8), are the main analytical results of this paper.

Next, we would like to find the condition for which the local charge changes from one atom to another in a periodic way. The relation equation (5) is expressed as a function of A_0^N; thus it should satisfy the same condition for the oscillations as the conductance. (The conductance can be expressed by means of A_0^N, [14].) We expect that for this condition the QW charge should behave in a special way, i.e. charge fluctuations (waves) with a fixed period or constant value of the charge can be observed. The relation for an M-atom period of the conductance can be written as follows [14]:

$$\cos\left(\frac{\pi l}{M}\right) = \frac{E-\varepsilon_0}{2V_N}, \qquad 0 < l < M. \tag{9}$$

This equation indicates the relation between $E-\varepsilon_0$ and V_N which leads to M-atom conductance oscillations and for example the even–odd oscillations, $M = 2$, are observed for $E - \varepsilon_0 = 0$. For a period equal to M one has $M - 1$ possible solutions of equation (9). It is interesting that when the conductance oscillates with a fixed period of M the following relation is satisfied: $\det B^{n-1}\det B^{N-n} \equiv \det B^{(n+M)-1}\det B^{N-(n+M)}$. This relation can be helpful in analysing the values of the LDOS for different atoms in the wire.

3. Results and discussion

In our calculations we put the Fermi energy as the reference energy point ($E_\mathrm{F} = 0$) and express all energies in units of Γ. Moreover, the zero temperature case is assumed.

3.1. Non-disturbed quantum wire

The knowledge of the wire density of states allows us to obtain for example the charge localized at QW atoms. In figure 1 we show the local density of states at the first atom, $n = 1$ (thick solid lines), and at $n = 2, 3$ atoms (thin solid and broken lines) for a wire which consists of $N = 6$ ($N = 7, 18$) atoms—upper panel (middle and lower panel, respectively). Here we put $V_N = 4$ and consider the case when the conductance oscillates with the period of four atoms, i.e. $\varepsilon_0^2 = 2V_N^2$. We observe non-zero values of the LDOS only for $E - \varepsilon_0 \leqslant 2V_N$—the electron band structure of the wire is limited to this region. Every LDOS is a symmetric function of the energy $E = \varepsilon_0$. Moreover, for an N-atom wire the LDOS of the nth atom is the same as that of the $(N-n+1)$th atom: for example, for $N = 6$ (upper panel) the LDOS for the $n = 1$ (2, 3)th

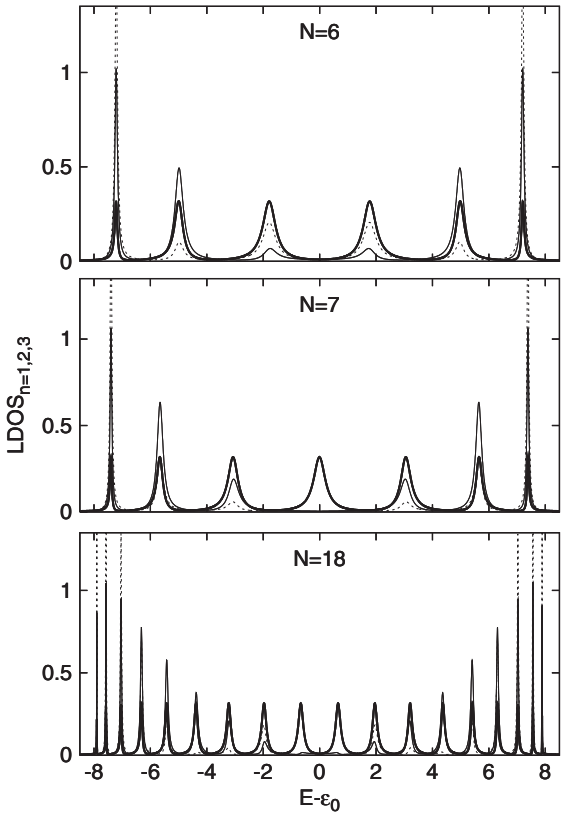

Figure 1. Local density of states at the $n = 1$ (2 and 3)th atom—thick solid lines (thin and broken lines, respectively) for the length of the quantum wire $N = 6$ (upper panel) for $\varepsilon_0 = -\sqrt{2}V_N$ and $V_N = 4$, $\Gamma = 1$. The middle (lower) panel corresponds to $N = 7$ ($N = 18$).

atom is the same as for $n = 6$ (5, 4)th atom, respectively. The symmetry of the LDOS results from the symmetric model of the wire coupled with leads. It is interesting that for an N-atom wire one observes N local maxima in the LDOS. For an odd number of atoms in the wire, the LDOS of every odd atom is characterized by a local maximum for $E - \varepsilon_0 = 0$, whereas for an even number N the LDOS is minimal for every atom—compare for example the upper and middle panels for $E - \varepsilon_0 = 0$ (in the case of $N = 7$ the LDOS of the $n = 1, 3, 5, 7$th atom possesses the same maximal value).

The heights of all LDOS peaks are different, depending on the position of the atom in the wire. Generally, we observe that for atoms which are at either ends of the wire the heights of LDOS peaks are more or less the same, whereas for atoms situated in the middle of the wire the edge LDOS peaks are much higher than in the middle of the energy band; compare the broken and thin solid lines. This effect is due to the connection between the wire and electrodes. The atoms which are close to one of the electrodes are characterized by wider LDOS peaks due to the Γ coupling. The influence of the electrodes on the middle QW atoms is smaller and this is the reason we observe rather high peaks in the LDOS for these atoms.

Here we would like to discuss the influence of the LDOS on the conductance through the system. It is known that for every odd-length QW, when the single electron energy ε_0 corresponds to the Fermi level, $E - \varepsilon_0 = 0$, the conductance is maximal. In this case, the

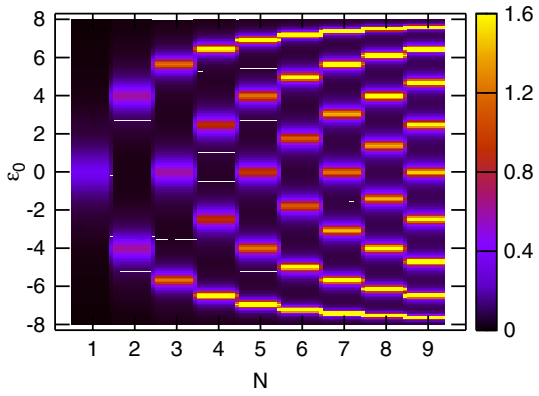

Figure 2. The total density of states at the Fermi level ($E_F = 0$) as a function of the wire's length, N, and ε_0. $\Gamma = 1$, $V_N = 4$.

electron tunnels through such wire but the LDOS at the Fermi energy is almost zero for every odd atom in the wire; for example for $N = 3$LDOS(E_F) is maximal for $n = 1, 3$ and is zero for $n = 2$. One can expect that in this case the LDOSs at the Fermi level should be maximal (or finite) for every atom in the wire, but this is not true. In this case the electron tunnels very quickly and spends very little time at each side. Thus according to the Heinsenberg uncertainty relation the indeterminancy of energy is rather large and the electron can tunnel through the LDOS peaks (side-bands) which are not at the Fermi level. For a wire which consists of an even number of atoms, the LDOS at the Fermi energy is almost zero for all atoms and the conductance is minimal. Here the possibility of the electron tunnelling from the lead to the first QW atom is very small due to almost zero value of the LDOSs. In that case the electron spends a rather long time in the electrode and its energy is very well determinate. Thus the electron cannot tunnel through the LDOS side bands.

In figure 2 the QW density of states as a function of the wire's length, N, and the single electron energy, ε_0, is shown: $\mathrm{DOS}_N = \sum_{i=1}^{n} \mathrm{LDOS}_i$—this corresponds to the total DOS of the system. As one expects, the periodic structure of DOS at the Fermi level is correlated with the conductance through the system—one can compare this picture with figure 1 in [14]. Here one can easily check the condition for the conductance oscillations, equation (9); for example, for $\varepsilon_0 = \pm V_N$ a three-atom period is observed. The heights of the local maxima in figure 2 increase with N because one has to sum the LDOS for more atoms. This figure shows that the knowledge of LDOS allows us to determine the conductance of the system (the LDOSs must be summed). The product of LDOS(E_F) for $N > 1$ is almost zero due to the above-mentioned minima of the LDOS at the Fermi level and is not linked with the conductance through the system at all. In that case one does not observe any oscillations like in figure 2.

Figure 3 presents the local charge localized at every atom of the wire—the lengths of the wire are as follows: $N = 1, 2, 3, 4$ (upper panel) $N = 5, 6, 7, 8, 10$ (middle panels) and $N = 18$ (lower panel). In this case we put $\varepsilon_0 = -\sqrt{2}V_N$, which leads to four-atom oscillations of the conductance. Let us analyse how the charge is distributed in the wire when the length of the wire is changed. For $N = 1$ (one-atom wire) the charge localized at the first atom Q_1 is indicated by the single star in the upper panel. For the two-atom wire ($N = 2$) we have $Q_1 = Q_2$ as we consider here the symmetric model. This symmetry is also visible for different N (see other panels), i.e. $Q_n = Q_{N-n+1}$. For the three-atom wire, $N = 3$, the charge at the middle atom Q_2 is lower than for edge atoms Q_1 and Q_3. A similar conclusion is also valid

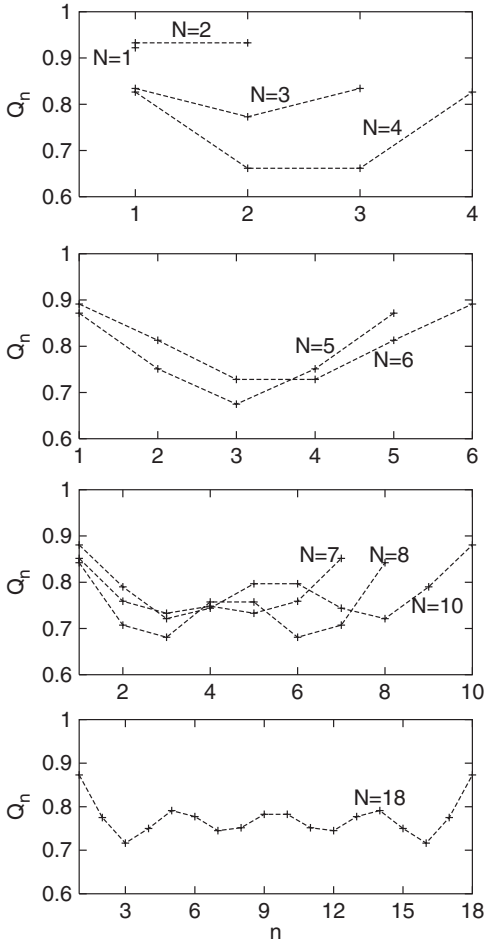

Figure 3. Local quantum dot charges at every atom for an $N = 1, 2, 3, 4, 5, 6, 7, 8, 10$ and 18 QW (from upper to lower panel) and for $\varepsilon_0 = -\sqrt{2}V_N$ and $V_N = 4$, $\Gamma = 1$. The lines are plotted for better visualization.

for $N = 4, 5, 6$. For $N = 7$ we observe the local maximum of the local charge for Q_4 and a similar behaviour is visible for $N = 8$ and 10—the maxima lead to oscillations of the charge localized in the wire. These oscillations (with a period of 4) are better visible for $N = 18$ (the lower panel). In that case the charge localized at atoms oscillates with the same period as the conductance. It is worth mentioning that we observe the conductance oscillations as a function of the wire length N, whereas the local charge oscillations are visible for a fixed length of the wire. It is expected that the formation of charge waves inside the wires can be confirmed experimentally. Few-atom wires consisting of a different number of atoms can be formed on vicinal surfaces, for example Au wires on vicinal Si surfaces [4–6]. The length of such wires depends mainly on the amount of deposited atoms. The knowledge of the LDOS at every atom (measured for example with the STM method) allows us to obtain the local charge. Thus the results shown in figure 3 can be simply verified.

In figure 4 we show the local charges localized at every atom of an $N = 18$ quantum wire ($n = 1, \ldots, 18$) for $V_N = 4$ and for $\varepsilon_0 = \pm V_N$ (thin solid lines), $\varepsilon_0 = \pm\sqrt{2}V_N$ (solid

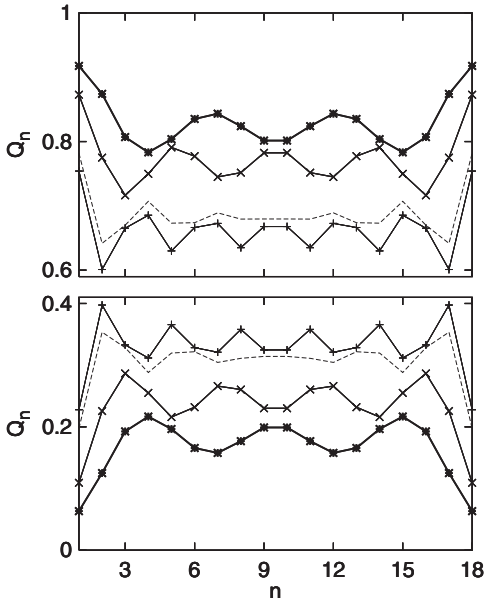

Figure 4. Charges localized at every atom for an $N = 18$ QW for $\varepsilon_0 = -V_N, -\sqrt{2}V_N, -\sqrt{3}V_N$ (thin solid, solid and thick solid lines, respectively)—upper panel. The lower panel corresponds to $\varepsilon_0 = +V_N, +\sqrt{2}V_N, +\sqrt{3}V_N$ (thin solid, solid and thick solid lines, respectively). $V_N = 4$, $\Gamma = 1$. The broken lines correspond to the non-resonant case $\varepsilon_0 = \pm 1.093 V_N$. The lines are plotted for better visualization.

lines) and for $\varepsilon_0 = \pm\sqrt{3}V_N$ (thick solid lines). Here the sign plus (minus) corresponds to the lower (upper) panel. The positions of ε_0 correspond to three-, four- and six-atom periods of the conductance oscillations, and as one can see, the same periods are observed in the local charges inside the wire. It is interesting that although we consider the same single-electron energies, ε_0, and the same hoppings between atoms, V_N, the charges localized at every QW atom are different and oscillate with n. These oscillations result from the structure of LDOS of the wire, i.e. for different atoms we observe different heights of the LDOS peaks. The broken lines in figure 4 correspond to $\varepsilon_0 = \pm 1.093 V_N$—near the three-atom period of the conductance (but out of this condition). In that case the local QW charge is not an oscillatory function of n although for $\varepsilon_0 = \pm V_N$ these oscillations are observed. It is worth mentioning that the amplitude of the charge waves inside the wire is maximal for end atoms and decreases for the middle ones. This suggests that the charge fluctuation effect is observed due to the reflection of an electron on the end of the wire. It was checked that these oscillations remain for very small Γ. The coupling parameter Γ influences the half-width of the LDOS peaks at the QW atoms and for finite Γ it is easier to numerically integrate the appropriate LDOS functions. The effects of charge fluctuations in low-dimensional systems have been observed experimentally (see e.g. [27, 28]) and were explained in terms of Friedel oscillations. The electron waves in two-dimensional systems are dramatically affected by small defect concentrations. Similarly, wire end atoms or wire–electrode connections play the same role, causing the formation of charge waves. These fluctuations inside the wire strongly depend on the relation between ε_0 and V_N and, as was mentioned above, for the non-resonant case (equation (9) is not satisfied) the charge waves disappear very quickly; see the broken line in figure 4.

One can conclude that the distribution of local charges in the wire is linked with the conductance oscillations and for an M-atom period of the conductance we observe inside that

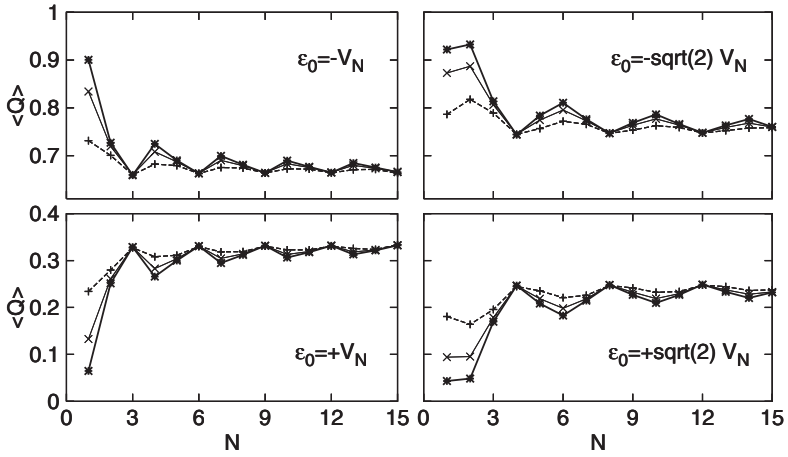

Figure 5. The average QW charge versus the length of the wire N for $V_N = 1, 2$ and 4 (broken, thin solid and thick solid lines) and for $\varepsilon_0 = \pm V_N$ ($\varepsilon_0 = \pm\sqrt{2}V_N$)—left panels (right panels). The lines are plotted for better visualization. $\Gamma = 1$.

wire a charge wave with period M. Here we do not consider the even–odd oscillations as in this case the LDOS at every QW atom is symmetrical versus the energy $E_F = \varepsilon_0 = 0$, and using equation (2) we obtain $Q_n = 0.5$ for $n = 1, \ldots, N$.

Now we analyse the case when the single electron energies ε_0 are localized below and above the Fermi energy (the upper and lower panel in figure 4, respectively). It can be seen that for $\varepsilon_0 < E_F$ ($\varepsilon_0 = -V_N, -\sqrt{2}V_N, -\sqrt{3}V_N$) the edge-atom occupations are higher than that for the middle atoms (upper panel). For $\varepsilon_0 > E_F$ (lower panel) the charges localized at the wire end atoms are lower than for the middle atoms. This leads to a very interesting result: for ε_0 localized above the Fermi energy the local charge curve possesses one maximum less than for ε_0 localized below E_F; for example, the thick solid line for $\varepsilon_0 = +\sqrt{3}V_N$ (lower panel) possesses three local maxima whereas for $\varepsilon_0 = -\sqrt{3}V_N$ (upper panel) there are four local maxima. It is worth mentioning that an STM investigation of Au wires on vicinal surfaces shows voltage-dependent oscillations of the distance between the STM peak and the surface. Moreover, the topography images show that the electron density of distribution between atoms strongly depends on the applied voltage and for example for a negative voltage one can see more peaks than for the positive voltage; see figure 1 in [5]. In an STM investigation the applied voltage between the STM tip and the surface can modify the position of the single electron energies ε_0 and this is the reason we observe different characteristics for positive and negative voltages; see also [6].

Next, in figure 5 we show the average QW charge as a function of the wire's length, N. The average charge of the wire is obtained from the following relation: $\langle Q \rangle = \sum_{n=1}^{N} Q_n/N$. The broken, thin solid and thick solid lines correspond to different coupling strengths between atoms, $V_N = 1, 2$ and 4, respectively. The left (right) panels correspond to the condition for the three (four)-atom period of the conductance, $\varepsilon_0 = \pm V_N$ ($\varepsilon_0 = \pm\sqrt{2}V_N$). The average charge of the wire in both cases depends on the position of ε_0 and for example for $\varepsilon_0 = -V_N$ (left upper panel) it tends to a constant value with increasing N, i.e. $\langle Q \rangle = 2/3$. Moreover, it oscillates with the same period as the conductance but the amplitude of these oscillations decreases very quickly with N. For $\varepsilon_0 = +V_N$ (left lower panel) we also observe that the amplitude of the average charge decreases with N and $\langle Q \rangle$ tends to the value $1/3$ for large N. Similar conclusions are valid for the case of four-atom conductance oscillations (right panels)

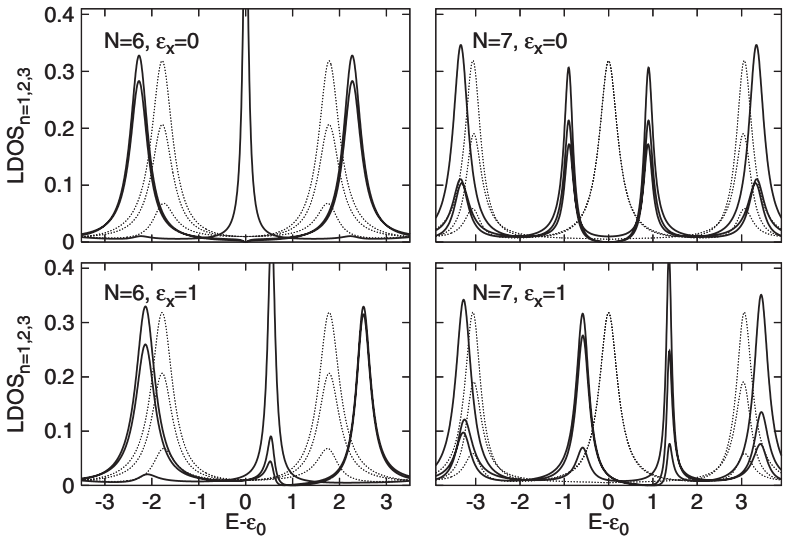

Figure 6. Local density of states at $n = 1$ (2 and 3) atom—thick solid lines for the length of the quantum wire $N = 6$ (left panels) and $N = 7$ (right panels) for $\varepsilon_0 = 0$ and $\varepsilon_x = 0$ (upper panels), $\varepsilon_x = 1$ (lower panels); $V_N = 4$, $\Gamma = 1$. The adatom connected to the first QW atom, $l = 1, t = 2$. The dotted lines correspond to LDOS for the non-disturbed wire.

and for other periods (not shown here). For $M = 4$ the average charge, with increasing N, tends to $3/4$ ($\varepsilon_0 = -\sqrt{2}V_N$, right upper panel) and $1/4$ ($\varepsilon_0 = +\sqrt{2}V_N$, right lower panel). In the case of four-atom oscillations the occupation $2/4$ is also possible but it appears for the condition $\varepsilon_0 = 0$ (even–odd conductance oscillations) which is a special case of every even-atom oscillation. It is a known effect that the occupation of an infinite wire is determined by the period of conductance oscillations [13, 14] and for period M we have $M - 1$ possible occupations of the wire: $1/M, 2/M, \ldots, (M-1)/M$. It is interesting that the average QW charge, for large N, is independent on the coupling strength V_N. The differences are visible only for not very long wires. Moreover, for strong value of V_N the average charge oscillations are more visible than for weak couplings.

The above conclusions suggest that one can influence the total charge localized at the finite and not very long wire by changing the distance between electrodes, for example by using the MCBJ method. In that method a few-atom wire can be formed between electrodes. One of these electrodes can vibrate or change its position (the coupling strength V_N is also changed) but the total number of atoms in the wire should remain unchanged. Thus, in this system one can detect the charge current because the average charge of a not very long wire depends on the coupling strength, V_N (and so on the distance between electrodes), as was shown in figure 5.

3.2. QW with side-attached adatom

Here we study the influence of a side-attached atom on the local density of states and charges in the wire. In figure 6 the LDOS at the first, the second and the third atom (thick lines) in a wire which consists of $N = 6$ (left panels) and $N = 7$ (right panels) atoms are shown. The dotted lines correspond to the wire which is non-disturbed by an adatom (plotted only for comparison between considered cases) and are the same as in figure 1. The additional atom is connected to the first QW atom but the results are also valid for connections with other QW atoms. The

upper panels correspond to the case when the single-electron energy of the adatom is the same as that of the QW atoms i.e. $\varepsilon_x = \varepsilon_0 = 0$. The lower panels are obtained for $\varepsilon_x = 1$. First, let us analyse the case $N = 6$ (an even number of atoms in the wire). For the non-disturbed wire the LDOSs at every QW atom are almost zero for $\varepsilon_0 = E_F = 0$ whereas in the presence of the adatom there is very high peak in the LDOS ($n = 2, 4$). Moreover, the distances between side-band peaks are wider when the adatom is connected to the wire. For an odd number of atoms in the wire, $N = 7$, the LDOSs of the non-disturbed wire at the sites $n = 1, 3, 5, 7$ are characterized by maximal values at the Fermi level. In the presence of the adatom the LDOS of every atom in the wire has a minimum at the Fermi level but there are two local symmetric maxima near this level (for each QW atom); see the solid lines in the upper right panel. The relative distance between these maxima depends on the coupling strength t (here $t = 2$). In the case when the adatom electron energy level is not equal to the electron energy of the QW atoms, i.e. $\varepsilon_0 \neq \varepsilon_x$, the situation is somewhat different. The local maxima for $N = 6$ are shifted versus the Fermi energy and minima in the LDOS appear for $E = \varepsilon_x$. For $N = 7$ the values of the LDOS for every atom in the wire are rather small but non-zero. For the energy $E = \varepsilon_x$, the LDOS at every odd atom in the wire, $n = 1, 3, 5, 7$, is equal to zero (for every even atom we observe a non-zero value of the LDOS). Moreover, the distance between side-band peaks is wider in comparison with the non-disturbed wire. Although we discuss here only the case of $N = 6$ and 7 the main features of the LDOS also remain valid for different N. It is worth mentioning that the LDOSs in the presence of an adatom ($\varepsilon_0 \neq \varepsilon_x$) are not symmetrical functions (versus $E - \varepsilon_0$) and also the LDOS of the nth QW atom is not the same as that of the $N - n + 1$th atom (this conclusion was satisfied for a non-disturbed wire). Thus we expect to observe non-symmetrical behaviour of the local charge inside a disturbed wire. It will be shown later that the charge waves are disturbed due to the adatom.

Generally speaking, an adatom changes the LDOS of a wire. For an even number of atoms in the wire the local maximum appears at the Fermi energy (when all atoms are the same kind) or near the Fermi energy (for different atoms). On the other hand, for an odd number of atoms in the wire the adatom blocks the LDOS at the Fermi level. In this case two local maxima appear near E_F. Moreover, the distance between LDOS peaks is somewhat larger for a disturbed wire. One can conclude that the adatom disturbs the LDOSs of the QW atoms and changes their values for the energy which corresponds to the adatom electron energy level. This means that in the presence of an adatom the electron transport through a wire and QW charges change their values, and thus it is possible to experimentally observe these effects.

In figure 7 the total density of states at the Fermi level, $\mathrm{DOS}_{N+1} = \sum_{i=1}^{N+1} \mathrm{LDOS}_i$, is shown as a function of the length of the wire, N, and the position of the single electron energy ε_0. The adatom is connected with the second QW atom, $l = 2$ and $\varepsilon_x = 1$, $t = 2$. The pattern of maxima and minima in the DOS of the system is shown in figure 7. In comparison with the results for a non-disturbed wire, figure 2, the symmetry of the DOS structure is broken. The main differences are visible for the region $\varepsilon_0 > 0$, i.e. for the energy which corresponds to ε_x. This conclusion is in agreement with the results from figure 6, where only the LDOSs were analysed. The upper light fields of maxima in figure 7 are shifted in comparison with figure 2 and causes the distance between maxima for fixed N to increase; compare this with the same effect in figure 6. The structure of the DOS for $\varepsilon_0 < 0$ remains almost unchanged in comparison with a wire without an adatom. The total DOS of a wire is connected with the conductance, see for example figure 2, and the results shown in figure 7 are proportional to the conductance of the wire disturbed by the adatom. Moreover, these results can be confirmed experimentally using the sharp-tip STM method (one has to measure and sum the LDOSs) or using the blunt-tip STM (one measures the density of states of all QW atoms; N must be rather small).

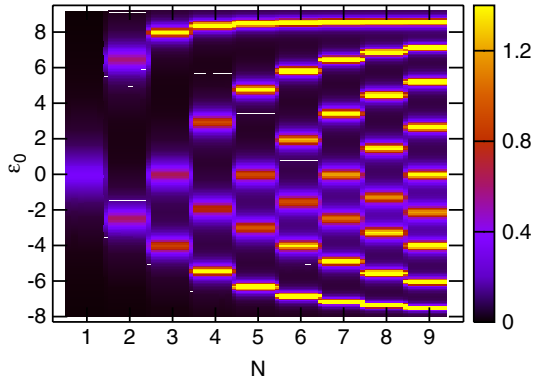

Figure 7. The total density of states at the Fermi level ($E_F = 0$) as a function of the wire's length, N, and ε_0 for $\varepsilon_x = 1$, $t = 2$, $l = 2$, $V_N = 4$, $\Gamma = 1$.

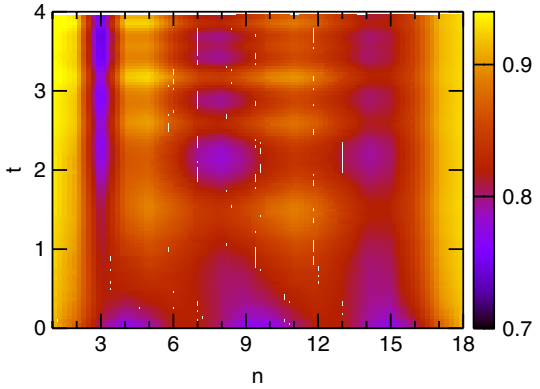

Figure 8. The charges localized at every atom for an $N = 18$ QW for $\varepsilon_0 = -\sqrt{3}V_N$ as a function of t; the other parameters are $l = 2$, $\varepsilon_x = 0$, and $V_N = 4$. The fields between integer n are plotted for better visualization.

Next, in figure 8 the local charge localized at every QW atom as a function of the coupling strength, t, is shown for $N = 18$, $V_N = 4$ and $\varepsilon_0 = \sqrt{3}V_N$ (the condition for a six-atom period). The adatom is connected with the third QW atom, $l = 3$. The fields between integer n are plotted for better visualization of the local charge surface. For $t = 0$ (non-disturbed wire) the result is the same as that presented in figure 4, the upper panel, thin solid line—the maxima of the local charge we observe for $n = 1, 7, 12$ and 18. For small coupling t the structure of the local charges in the wire is almost unchanged. For greater value of t the local charge at the third QW atom decreases and the local minimum is observed for $n = 3$. Moreover, the local maximum appears for $n = 4$—in the case of $t = 0$ the local minimum is for $n = 4$. The local charges localized at others QW atoms remain more or less the same. The main differences are observed for the atom which is connected with the adatom or at atoms which are situated very close to this atom. In conclusion, the additional atom causes a disturbance of the local charge at the QW atom which is connected with the adatom. Thus the charge fluctuations (waves) along the wire in the presence of the adatom are not symmetrical in comparison with a non-disturbed chain. These results are also valid for different positions of the adatom at the wire.

4. Conclusions

In summary, using the tight-binding Hamiltonian and retarded Green function formalism the local and total density of states and the charges of a QW were obtained for a perfect and a disturbed wire. The same single electron energies of all atoms, ε_0, and the same nearest-neighbour interactions, V_N, in the wire were assumed. The electron–electron interactions inside the wire, U, were not taken into consideration. In the presence of a rather weak U and under the Hartree–Fock approximation charge waves can be observed in the system (for $U = 0$ they exist). Moreover, as was shown in [18] the conductance oscillations also remain for $U \to \infty$ and (because these oscillations are linked with the charge waves inside the wire) it is expected that for the finite U the fluctuations of the charge can also be observed especially in the paramagnetic configuration. As concerns the ferromagnetic case, charge waves can exist (the Friedel oscillations in a one-dimensional fermion system exist, [29]) but it is difficult to predict the behaviour of spin-up and spin-down charges inside the wire. The problem will be further studied.

The main results of this paper can be summarized as follows.

(1) An analytical formula for the local density of states at every QW atom in a wire with side-attached adatom was obtained, equation (5), and discussed.
(2) The LDOSs inside a wire which consists of an even number of atoms are characterized by local minima for $E - \varepsilon_0 = 0$ (for every QW atom) but in the presence of an adatom there are maxima in the LDOSs, depending on the position of ε_x; compare figures 1 and 6. Moreover, the structure of the total DOS is characterized by the local minima and maxima, and for a non-disturbed wire its structure is fully symmetric. The adatom causes a disturbance in this symmetry especially for the energy which corresponds to the single electron energy of the adatom; compare figures 2 and 7.
(3) The period of the charge waves is correlated with the period of the conductance oscillations. Charge waves are observed in a finite wire for the case when the condition for the conductance to oscillate is satisfied. For the case when this condition is not satisfied charge waves are not observed; compare figures 3 and 4. In the presence of an adatom the oscillations of the local charge are disturbed and the main differences in the charge are observed for the QW atom directly connected with the adatom.
(4) For the single electron energies, ε_0, localized above the Fermi energy the local charge curve (the local charges at the QW atoms) possesses one maximum less than for ε_0 localized below E_F; see figure 4.

It is believed that the results presented in this work can be confirmed experimentally using the STM or MCBJ methods. They can also be useful in nanoelectronics as the monatomic chain is the thinnest possible electric wire. Moreover, one can use the conclusions of this paper to interpret the STM pictures of one-dimensional systems where a different number of peaks are observed for different voltage polarizations.

Acknowledgments

This work has been supported by KBN grant No 1 P03B 004 28 and the Foundation for Polish Science. The author thanks Dr Mariusz Krawiec for helpful discussions.

References

[1] Yazdani A, Eigler D M and Lang N D 1996 *Science* **272** 1921
[2] Smit R H M, Untiedt C, Rubio-Bollinger G, Segers R C and van Ruitenbeek J M 2003 *Phys. Rev. Lett.* **91** 076805

[3] Agrait N, Yeyati A L and van Ruitenbeek J M 2003 *Phys. Rep.* **377** 81
[4] Jałochowski M, Stróżak M and Zdyb R 1997 *Surf. Sci.* **375** 203
[5] Krawiec M, Kwapiński T and Jałochowski M 2005 *Phys. Status Solidi* b **242** 332
[6] Krawiec M, Kwapiński T and Jałochowski M 2006 *Phys. Rev.* B **73** 075415
[7] Robinson I K, Bennett P A and Himpsel F J 2002 *Phys. Rev. Lett.* **88** 096104
[8] Lang N D 1997 *Phys. Rev. Lett.* **79** 1357
[9] Lang N D and Avouris Ph 1998 *Phys. Rev. Lett.* **81** 3515
[10] Kim T-S and Hershfield S 2002 *Phys. Rev.* B **65** 214526
[11] Sim H-S, Lee H-W and Chang K J 2001 *Phys. Rev. Lett.* **87** 096803
[12] Zeng Z Y and Claro F 2002 *Phys. Rev.* B **65** 193405
[13] Thygesen K S and Jacobsen K W 2003 *Phys. Rev. Lett.* **91** 146801
[14] Kwapiński T 2005 *J. Phys.: Condens. Matter* **17** 5849
[15] Auslaender O M *et al* 2005 *Science* **308** 88
[16] Thomas K J *et al* 1996 *Phys. Rev. Lett.* **77** 135
[17] Kane B E *et al* 1998 *Appl. Phys. Lett.* **72** 3506
[18] Krawiec M and Kwapiński T 2006 *Surf. Sci.* **600** 1697
[19] Wees B J *et al* 1988 *Phys. Rev. Lett.* **60** 848
[20] Thygesen K S, Bollinger M and Jacobsen K W 2003 *Phys. Rev.* B **67** 115404
[21] Thijssen W H A, Marjenburgh D, Bremmer R H and van Ruitenbeek J M 2006 *Phys. Rev. Lett.* **96** 026806
[22] Pouthier V and Girardet C 2002 *Surf. Sci.* **511** 203
[23] Orellana P A, Dominguez-Adame F, Gomez I and Ladron de Guevara M L 2003 *Phys. Rev.* B **67** 085321
[24] Lee Y J, Brandbyge M, Puska M J, Taylor J, Stokbro K and Nieminen R M 2004 *Phys. Rev.* B **69** 125409
[25] Datta S and Tian W 1997 *Phys. Rev.* B **55** 1914
[26] Mares A I, Otte A F, Soukiassian L G, Smit R H M and van Ruitenbeek J M 2004 *Phys. Rev.* B **70** 073401
[27] Kanisawa K, Butcher M J, Yamaguchi H and Hirayama Y 2001 *Phys. Rev. Lett.* **86** 3384
[28] Kanisawa K, Butcher M J, Tokura Y, Yamaguchi H and Hirayama Y 2001 *Phys. Rev. Lett.* **87** 196804
[29] Egger R and Grabert H 1995 *Phys. Rev. Lett.* **75** 3505